12-14-2017

Similar ultrafast dynamics of several dissimilar Dirac and Weyl semimetals

Christopher P. Weber
Santa Clara University, cweber@scu.edu

Bryan S. Berggren

Madison G. Masten

Thomas C. Ogloza

Skylar Deckoff-Jones

See next page for additional authors

Recommended Citation

Weber, C. P., Berggren, B. S., Masten, M. G., Ogloza, T. C., Deckoff-Jones, S., Madéo, J., Man, M. K. L., Dani, K. M., Zhao, L. X., Chen, G. F., Liu, J. Mao, Z. Q., Schoop, L. M., Lotsch, B. V., Parkin, S. S. P., and Ali, M. "Similar ultrafast dynamics of several dissimilar Dirac and Weyl semimetals", Journal of Applied Physics 122 22 (2017). https://aip.scitation.org/doi/10.1063/1.5006934

Authors
Christopher P. Weber, Bryan S. Berggren, Madison G. Masten, Thomas C. Ogloza, Skylar Deckoff-Jones, Julien Madéo, Michael K. L. Man, Keshav M. Dani, Lingxiao Zhao, Genfu Chen, Jinyu Liu, Zhiqiang Mao, Leslie M. Schoop, Bettina V. Lotsch, Stuart S. P. Parkin, and Mazhar Ali

Similar ultrafast dynamics of several dissimilar Dirac and Weyl semimetals

Chris P. Weber, Bryan S. Berggren, Madison G. Masten, Thomas C. Ogloza, Skylar Deckoff-Jones, Julien Madéo, Michael K. L. Man, Keshav M. Dani, Lingxiao Zhao, Genfu Chen, Jinyu Liu, Zhiqiang Mao, Leslie M. Schoop, Bettina V. Lotsch, Stuart S. P. Parkin, and Mazhar Ali

Citation: Journal of Applied Physics **122**, 223102 (2017); doi: 10.1063/1.5006934

View online: https://doi.org/10.1063/1.5006934

View Table of Contents: http://aip.scitation.org/toc/jap/122/22

Published by the American Institute of Physics

Similar ultrafast dynamics of several dissimilar Dirac and Weyl semimetals

Chris P. Weber,[1,a)] Bryan S. Berggren,[1] Madison G. Masten,[1] Thomas C. Ogloza,[1] Skylar Deckoff-Jones,[2] Julien Madéo,[2] Michael K. L. Man,[2] Keshav M. Dani,[2] Lingxiao Zhao,[3] Genfu Chen,[3] Jinyu Liu,[4] Zhiqiang Mao,[4] Leslie M. Schoop,[5] Bettina V. Lotsch,[5,6] Stuart S. P. Parkin,[7] and Mazhar Ali[7]

[1]*Department of Physics, Santa Clara University, 500 El Camino Real, Santa Clara, California 95053-0315, USA*
[2]*Femtosecond Spectroscopy Unit, Okinawa Institute of Science and Technology Graduate University, 1919-1 Tancha, Onna-son, Kunigami, Okinawa 904-495, Japan*
[3]*Institute of Physics and Beijing National Laboratory for Condensed Matter Physics, Chinese Academy of Sciences, Beijing 100190, China*
[4]*Department of Physics and Engineering Physics, Tulane University, New Orleans, Louisiana 70118, USA*
[5]*Max Planck Institute for Solid State Research, Heisenbergstasse 1, 70569 Stuttgart, Germany*
[6]*Department of Chemistry, Ludwig-Maximilians-Universität München, Butenandtstrasse 5-13, 81377 München, Germany*
[7]*Max Planck Institute of Microstructure Physics, Weinberg 2, 06120 Halle, Germany*

(Received 28 September 2017; accepted 15 November 2017; published online 8 December 2017)

Recent years have seen the rapid discovery of solids whose low-energy electrons have a massless, linear dispersion, such as Weyl, line-node, and Dirac semimetals. The remarkable optical properties predicted in these materials show their versatile potential for optoelectronic uses. However, little is known of their response in the picoseconds after absorbing a photon. Here, we measure the ultrafast dynamics of four materials that share non-trivial band structure topology but that differ chemically, structurally, and in their low-energy band structures: ZrSiS, which hosts a Dirac line node and Dirac points; TaAs and NbP, which are Weyl semimetals; and $Sr_{1-y}Mn_{1-z}Sb_2$, in which Dirac fermions coexist with broken time-reversal symmetry. After photoexcitation by a short pulse, all four relax in two stages, first sub-picosecond and then few-picosecond. Their rapid relaxation suggests that these and related materials may be suited for optical switches and fast infrared detectors. The complex change of refractive index shows that photoexcited carrier populations persist for a few picoseconds. *Published by AIP Publishing*. https://doi.org/10.1063/1.5006934

I. INTRODUCTION

Interest has surged lately in topological, three-dimensional semimetals whose low-energy electron dispersions are linear and cross masslessly at a node. Several classes of such relativistic semimetals have been proposed, including line-node,[1] Dirac,[2] and Weyl.[3,4] Subsequently, Weyl nodes were predicted in a family of monopnictides,[5,6] and discovered in TaAs.[7–9] Beyond their fundamental interest, such materials could be technologically useful: They typically display high mobility and large magnetoresistance.[10–14] It has been suggested that a *p-n-p* junction of Weyl materials could act as a transistor despite the lack of an energy gap[15] and that the materials could exhibit a large spin-Hall angle[16] and be ingredients in a quantum amplifier or a chiral battery.[17] Their potential for optical and optoelectronic uses are enhanced by exotic predicted effects such as photocurrent driven by circularly-polarized mid-IR light,[18] anisotropic photoconductivity,[19] optical conductivity that takes the form of a step-function tunable by external fields,[20] resonant transparency at THz frequencies tuned by a magnetic field,[21] and a mid-IR passband, tuned by the Fermi energy and lying between E_F and $2E_F$.[22]

Knowledge of a material's sub- and few-picosecond response to optical excitation—its ultrafast dynamics—holds practical significance. It reveals properties of the hot electrons important in high-field devices. More directly, it can guide optoelectronic applications: Recently, several devices have been reported that rely on the ultrafast properties of Cd_3As_2, the archetypal three-dimensional Dirac semimetal, to make fast photodetectors[23,24] and optical switches.[25] The monopnictide Weyl materials TaAs, TaP, and NbAs also show technological promise due to their sizable, anisotropic nonlinear-optical response.[26] Additionally, a broadband photodetector has recently been made out of TaAs.[27] The burgeoning variety of Dirac and Weyl semimetals, of diverse crystal and chemical structures, presents ever-wider opportunities for the materials' optoelectronic use; the need to explore and understand their ultrafast dynamics has grown commensurately. Knowledge of the materials' response to photoexcitation will likewise be important in realizing a predicted exciton condensate,[28] or various proposed effects in which intense pulses of light might separate or merge pairs of Weyl points or convert line nodes to point nodes.[29–32]

From recent ultrafast measurements on Cd_3As_2,[33–35] a picture is emerging in which its response to visible or near-infrared illumination is much like graphene's. Most electrons and holes are excited far from the Fermi energy, where the density of states is high [Fig. 1(b)]. In tens or hundreds of

a)Electronic mail: cweber@scu.edu

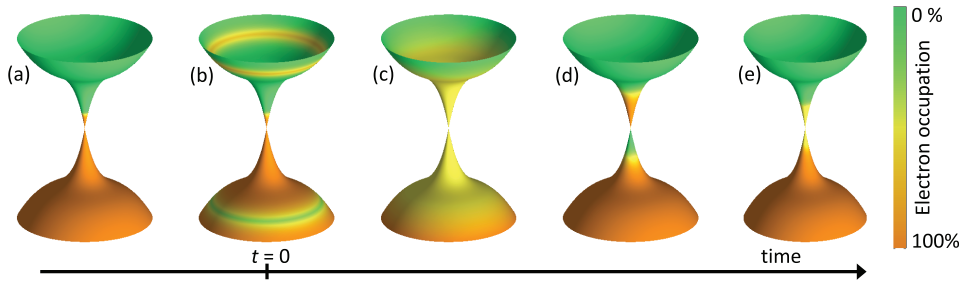

FIG. 1. Schematic representation of the excitation and relaxation of electrons and holes in Cd_3As_2, shown as a function of time after photoexcitation, left to right. The many trivial bands far from the Fermi energy are represented by a single, broad continuum. (a) Prior to excitation, the material is slightly *n*-type. (b) Electrons and holes excited at high energy. (c) A high-temperature thermal distribution. (d) A partially cooled distribution with inverted populations; it is unclear whether this situation occurs in Cd_3As_2. (e) A partially cooled, non-inverted distribution; so long as the electronic temperature T_e exceeds the lattice temperature, the carrier population remains thermally enhanced.

femtoseconds, they share energy among themselves and with the resident charge-carriers to produce a quasi-thermal distribution [Fig. 1(c)] whose temperature, T_e, exceeds the lattice temperature; many of them occupy the Dirac cone. As the carriers cool [Figs. 1(d)–1(e)], the narrowing of the Fermi-Dirac distribution further reduces the number of electrons and holes. In graphene, after forming the initial quasi-thermal distribution, electrons and holes may have separate chemical potentials[36,37]—that is, the carrier population may briefly be inverted [Fig. 1(d)]—recombining within a few hundred femtoseconds. Such inversion requires that the photocarriers' rate of cooling exceeds their recombination rate, and appears to be aided by the low density of states near the Fermi energy; indeed, it also occurs in the semimetals bismuth[38] and graphite.[39] In Cd_3As_2, however, it is not known whether a population inversion is ever formed.

Topological insulators (TIs) host surface states with a Dirac dispersion like that of the Dirac and Weyl semimetals. However, the ultrafast dynamics of these surface states are not closely analogous to those of the Dirac and Weyl semimetals, but instead are largely controlled by interactions between the bulk electronic states, which are gapped, and the surface.[40–42] Optical excitation populates bulk states; a metastable population of these bulk electrons gradually feeds the population of the surface state; and the cooling of electrons in the surface state is strongly influenced by bulk-surface coupling.

In three-dimensional Dirac semimetals other than Cd_3As_2, time- and angle-resolved photoemission experiments support the same picture as in Cd_3As_2. In the Weyl material $MoTe_2$,[43] and the gapped Dirac materials $ZrTe_5$,[44] and $SrMnBi_2$,[45] electrons excited by 1.5-eV photons relax into the Dirac cone within about 0.4 ps. The final stage of electronic cooling in $SrMnBi_2$ slows to a power law,[45] consistent with predictions for Dirac and Weyl semimetals.[46,47] In $MoTe_2$, the electrons' non-equilibrium temperature was seen to recover as a biexponential, with time constants 0.43 ps and 4.1 ps; in contrast to graphene, the population inversion illustrated in Fig. 1(d) was not observed.[43]

However, the most widespread measure of the ultrafast response, and that employed in this work, is the pump-induced change in reflectivity, $\Delta R(t)$, of a time-delayed probe pulse. While photoemission measures carrier populations near the Fermi energy, reflectivity measures changes in the index of refraction at the probe energy. This energy is well beyond the Dirac cone, but through the Kramers-Kronig relation $\Delta R(t)$ measures carrier populations at many energies. Indeed, work on Cd_3As_2 has shown that $\Delta R(t)$ primarily reveals the lifetime of the carriers near the Dirac point: The timescale of the ultrafast response was nearly independent of the probe photons' energy, but its magnitude increased as the probe's energy was lowered toward the Fermi level.[34] The materials' optoelectronic properties thus persist from the visible through the mid-infrared.[23,25]

In this work, we investigate the ultrafast dynamics of four Dirac and Weyl materials: TaAs and NbP;[5,12] ZrSiS;[48] and $Sr_{1-y}Mn_{1-z}Sb_2$.[49] As shown in Fig. 2, these materials differ sharply in chemical and crystal structure. TaAs and NbP crystallize in space group $I4_1md$, (#109) which can be thought of as a network of face- and edge-sharing $TaAs_6$ (or NbP_6) trigonal prisms. $SrMnSb_2$ ($Pnma$, #62) has layers of edge-sharing $MnSb_4$ tetrahedra spaced by a bilayer of face-sharing $SrSb_8$ square antiprisms. In the shared Sb layer, the Sb atoms are distorted from square nets to form zig-zag chains. This contrasts with ZrSiS ($P4/nmm$ #129), which can be thought of as layers of mono-capped square antiprisms with Zr coordinated by Si and S with the Si atoms forming a planar square net between Zr layers. The materials' one common feature is that their electronic structures, near E_F, have linear band crossings and a local minimum in the density of states—even though these differ in origin and type. ZrSiS is a Dirac line-node semimetal and, by virtue of having both inversion and time-reversal symmetry, has Dirac nodes near E_F that are gapped to a small extent by spin-orbit coupling.[48] TaAs and NbP are inversion-breaking Weyl semimetals, resulting in doubly degenerate Weyl points near E_F,[5,6] and negative magnetoresistance induced by the chiral anomaly has been observed in TaAs.[12] $Sr_{1-y}Mn_{1-z}Sb_2$ preserves inversion symmetry but breaks time-reversal symmetry due to magnetic ordering. The Sb plane gives rise to nearly massless Dirac fermions.[49]

As our experiments reveal, these four dissimilar materials share very similar ultrafast responses, consisting of sub-picosecond and few-picosecond components. Moreover, the results of our phase-sensitive transient-grating measurements indicate that a carrier population lasts for at least 1ps. These four materials' responses are similar to those of Cd_3As_2, but even faster, suggesting that they, too, may be well-suited for

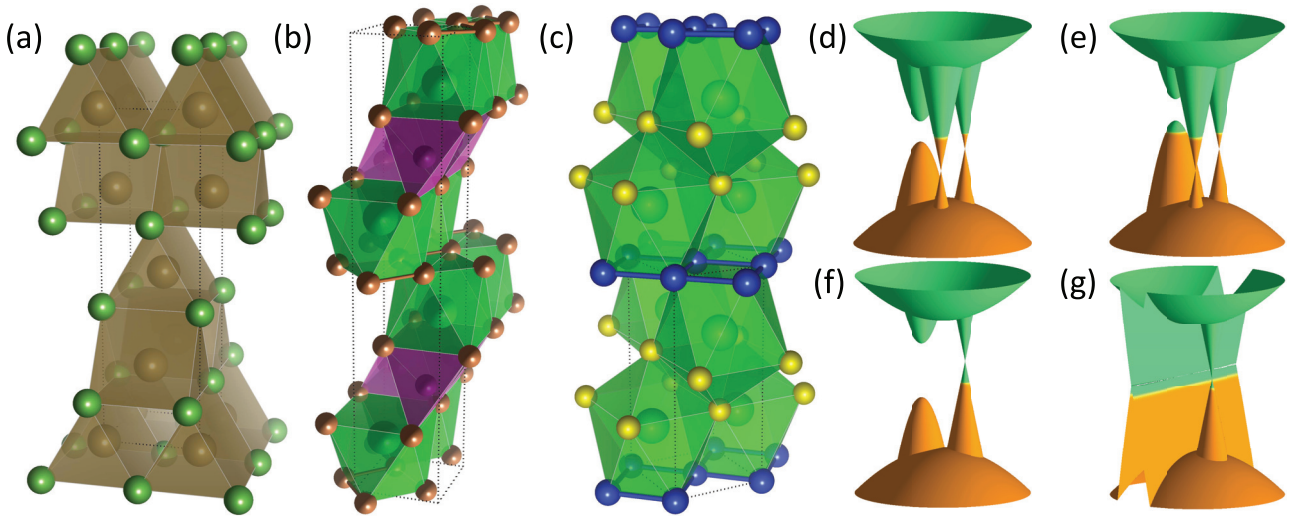

FIG. 2. Crystal and band structures. (a)–(c) Crystal structures. (a) TaAs and NbP. Shown are the As_6 (or P_6) prisms, with a single Ta (or Nb) at the center of each. (b) $SrMnSb_2$, with Sb atoms shown in brown. The Sb_4 tetrahedra (magenta) each contains a Mn atom, while the Sb_8 square antiprisms (green) each contains an Sr atom. (c) ZrSiS, with Si in blue and S in yellow. Each mono-capped square antiprism consists of a Zr atom coordinated by four Si atoms forming a planar square net and five S atoms. (d)–(g): Schematic low-energy band structures. The many trivial bands far from the Fermi energy are represented by a single, broad continuum. Features that occur at many points in the Brillouin zone are shown just once; chirality is not indicated. Filled and empty states are indicated in the same color-scale as Fig. 1. (d) In TaAs, there are *n*-type linear cones of two different energies. (e) NbP has a band structure like that of TaAs, but a different Fermi level introduces *p*-type massive carriers. (f) In $Sr_{1-y}Mn_{1-z}Sb_2$ transport is dominated by a *p*-type linear cone. (g) ZrSiS, showing a line node and a Dirac cone (both shown *p*-type).

optical switches and photodetectors. As the discovery of additional Dirac and Weyl semimetals proceeds, other materials are likely to follow the same pattern and therefore to enable a wide range of optoelectronic applications.

II. METHODS

The single crystals of TaAs were grown by the chemical vapor transport method, which was described in Ref. 12. Samples grown in this way show electronic mobility reaching 1.8×10^5 cm^2/Vs at 1.8 K. The samples of $Sr_{1-y}Mn_{1-z}Sb_2$ were grown using a self-flux method as detailed in Ref. 49. They were "Type B," in the terminology of Ref. 49, with $y \approx 0.06$, $z \approx 0.08$, about 0.08 μ_B per Mn and a mobility near 10^4 cm^2/Vs. SdH oscillations on a sample from this batch had a frequency in the range of 66–70 T, corresponding to a very small Fermi surface with $A_F = 0.64\,\text{nm}^{-2}$. Transport is hole-dominated. This type of sample harbors nearly massless Dirac fermions. Single crystals of ZrSiS and NbP were both grown via iodine vapor transport. For ZrSiS, the synthesis followed the method of Ref. 48. For NbP, single crystals were grown from a polycrystalline powder of NbP (obtained from direct reaction of Nb and P at 800 °C for five days) at 950 °C with a temperature gradient of 100 °C. The crystals were obtained towards the hot end of the tube and then annealed at 500 °C for one week.

All ultrafast measurements used mode-locked Ti:Sapphire lasers [or, in Fig. 3(f), a fiber laser]. For the measurements at high fluence and wavelengths other than 800 nm [Figs. 3(e) and 4(a)], a long-cavity laser and optical parametric amplifier were used, and the beams were focused on the sample through a microscope objective. In Fig. 4(d), we determine the complex phase of $\Delta n(t)$ from a pair of transient-grating measurements by the method described in Refs. 33 and 50, and in the supplementary material Sec. S1, and using calculations of the static index n found in Ref. 51. All measurements used standard chopping and lock-in detection.

III. RESULTS

A. Ultrafast response

After a sample absorbs a short pulse of light, the "pump," we probe the dynamics of the photoexcited electrons by measuring the pump-induced change in the reflectivity, $\Delta R(t)$, of a "probe" pulse that arrives a time t after the pump. We also perform transient-grating measurements, an extension of the pump-probe method in which the diffraction of the probe is measured. For our purposes, the transient grating's significance lies primarily in improved signal. It is also phase-sensitive, measuring the real and imaginary parts of the change in reflectance, $\Delta r(t)$, where $R = rr^*$. While $\Delta r(t)$ is typically known only up to an overall complex phase of $e^{i\phi}$, we will show [in Fig. 4(d)] a measurement of ϕ that allows us to determine the change in the index of refraction, $\Delta n(t)$.

Examples of the transient-grating data appear in Fig. 3. Each material's $\Delta r(t)$ appears to have a different shape, but the differences lie mostly in the arbitrary phase ϕ and in the size of a nearly constant component that represents heating of the lattice (discussed below; also see supplementary material Sec. S2, Fig. S3, and Table S1). For instance, the real part of the NbP signal first dips then rises; but for a different phase ϕ it would first rise then fall, resembling TaAs.

Despite the differences of shape, it is the similarities in the materials' dynamics that are much more striking—along with their similarities to prior measurements of Cd_3As_2.[33] For each material, the ultrafast response on the timescale of interest fits well to a biexponential plus a constant

$$\Delta r(t) = Ae^{i\theta_A}e^{-t/\tau_A} + Be^{i\theta_B}e^{-t/\tau_B} + Ce^{i\theta_C}, \qquad (1)$$

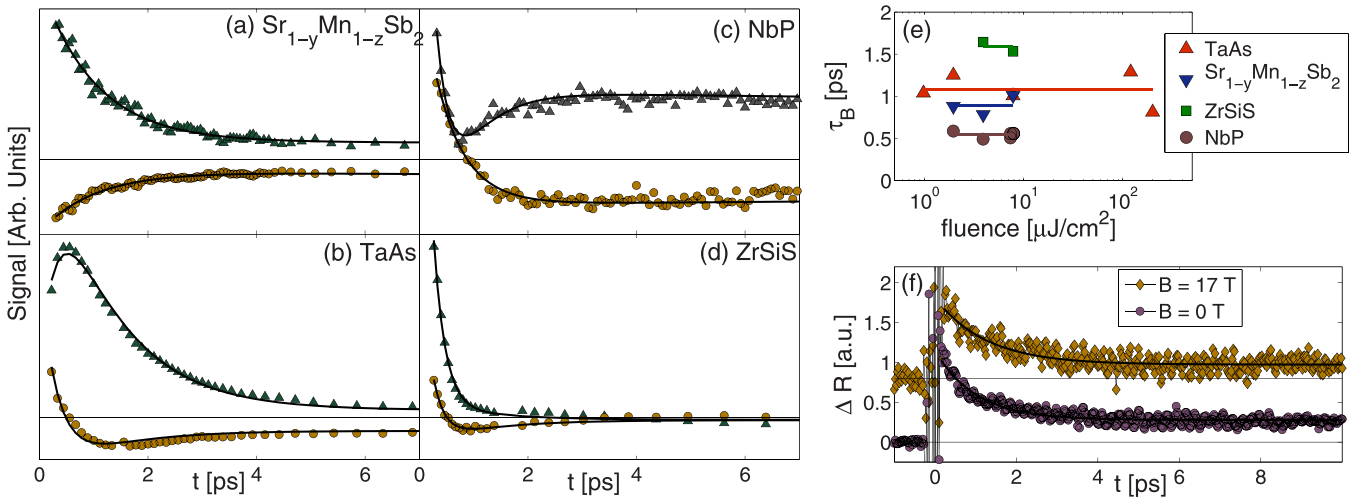

FIG. 3. Ultrafast responses. (a)–(d): Typical transient-grating data at room temperature for the four materials studied. Triangles and circles are real and imaginary parts, respectively (up to a factor of $e^{i\phi}$). Solid curves are fits to Eq. (1). (e) Fluence-dependence of the τ_B decay at room temperature. The two highest-fluence points for TaAs are measured with the probe energy below the pump; see Fig. 4(a). (f): $Sr_{1-y}Mn_{1-z}Sb_2$: 0 T (circles), 17 T (diamonds), both 10 K. Shifted for clarity. What looks like scatter in the data is actually oscillations. The smooth curves are fits to a single exponential plus an offset, and give τ_B of 1 ps and 1.3 ps, respectively. This experiment was pump-probe but not transient-grating, and thus measured $\Delta R(t)$, which is real-valued.

with τ_A sub-picosecond and τ_B several times longer (see Table I). The slower decay has an amplitude typically about 20% that of the fast one. (We found that attempts to fit the data to simpler functions such as a single exponential or a bimolecular decay were unsuccessful; see supplementary material Sec. S3 and Fig. S4).

Another similarity among these materials, and a similarity to Cd_3As_2, is that the ultrafast response is nearly independent of many experimental conditions. For all four materials, we see no difference between measurements at room temperature and at 10 K. For TaAs, we also measured temperatures from 80 to 230 K, a range over which the carrier densities n and p change by factors of 20;[52] nonetheless, τ_A and τ_B remained constant. The fluence, or energy per area, of the pump pulse also does not change the decay rate [Fig. 3(e)]. For $Sr_{1-y}Mn_{1-z}Sb_2$, we measured up to $B = 17$ T, with little or no change in the signal [Fig. 3(f)]; magnetic field likewise had no effect on the responses of TaAs (see supplementary material Sec. S4 and Fig. S5) or ZrSiS, though measured only up to $B = 0.3$ T. Naturally, the materials' responses do have some differences: Cd_3As_2 is the slowest, and NbP is the fastest; TaAs has a larger amplitude ratio B/A; NbP has the largest lattice-heating term. For $Sr_{1-y}Mn_{1-z}Sb_2$, the signal includes oscillations at a few THz, which overlap with the timescale of the fast decay and prevent us from determining τ_A. (These oscillations will be discussed in a separate publication.) Nonetheless, the very fast, two-part responses are notably similar for such dissimilar materials, contrasting both with other types of semimetal and with metals, as we discuss below. This similarity raises the hope that such a sub-picosecond and few-picosecond response may be generic to Dirac and Weyl materials, including those yet to be explored.

B. Physical origins of the ultrafast response

A full accounting of the many processes leading to the relaxation on timescales τ_A and τ_B in these four materials

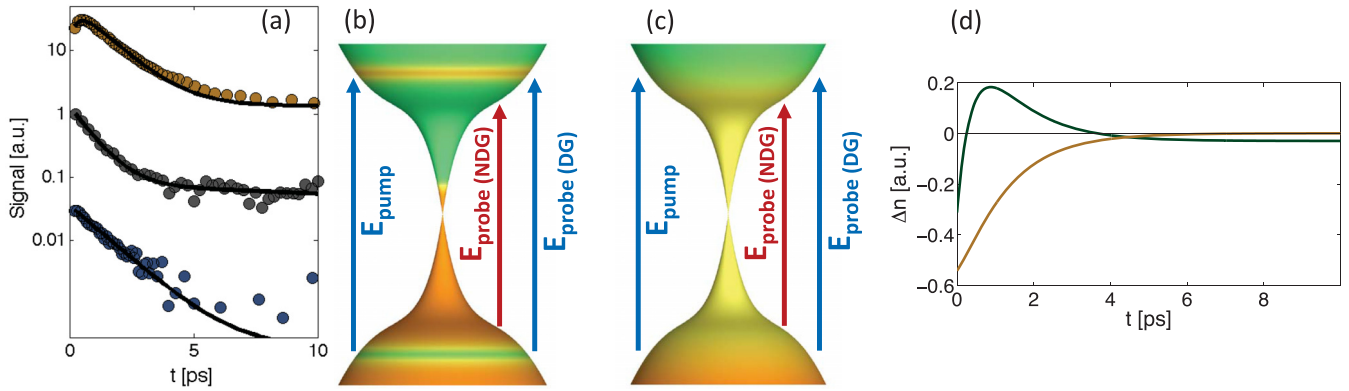

FIG. 4. Data for TaAs at room temperature. (a) Ultrafast response for various pump and probe energies. Top: pump 1.55 eV, probe 1.55 eV. Middle: pump 1.55 eV, probe 1.10 eV. Bottom: pump 2.36 eV, probe 1.55 eV. The curves are shifted vertically for clarity. The data are $\Delta R(t)$, which is real-valued. (b) and (c) Schematic illustration of the photon energies used as pump (blue) and probe in degenerate (DG) and non-degenerate (NDG) experiments, along with the electron occupation before (b) and after (c) interband scattering. (d) The photoinduced change in refractive index, $\Delta n(t)$; the real part is green, and the imaginary part is orange. The curve is calculated from the measured phase of $\Delta r(t)$ and from the data's fit to Eq. (1), as explained in Ref. 33.

TABLE I. Room-temperature decay rates for the materials studied. Rapid oscillations in the signal of $Sr_{1-y}Mn_{1-z}Sb_2$ make it impossible to determine τ_A.

Material	$Sr_{1-y}Mn_{1-z}Sb_2$	TaAs	NbP	ZrSiS	Cd_3As_2 (Ref. 33)
τ_A (ps)	*N/A*	0.38 ± 0.13	0.27 ± 0.06	0.19 ± 0.03	0.50 ± 0.04
τ_B (ps)	0.96 ± 0.18	1.1 ± 0.1	0.50 ± 0.08	1.6 ± 0.3	3.1 ± 0.1

would require many more experiments. However, the broad outlines of the processes are apparent.

First, consider the excitation of electrons and holes by absorption of pump photons of energy 1.55 eV, an energy that exceeds the extent of the Dirac or Weyl cones. The dominant optical transitions will be those with the largest joint density of states, and in semimetals, the density of states may be several orders of magnitude smaller near E_F than at higher and lower energies.[38] The pump therefore initially excites carriers into the massive bands beyond the range of the linear dispersion, as illustrated in Fig. 1(b).

The fast process we observe, τ_A, most likely arises from the scattering of electrons and holes out of these initial high-energy states. The electrons and holes form a "hot" distribution spread over a broad energy range and have temperatures that greatly exceed the lattice temperature [Fig. 1(c)]. The scattering may be both intraband and interband, and may include electron-electron and electron-phonon processes, both of which are hastened by the large density of states far from E_F. Additionally, electron-electron scattering is faster in semimetals than in metals because the Coulomb interaction is less screened.

Most of our experiments are "degenerate," with the pump and probe photons having the same energy of 1.55 eV. To confirm that most carriers lie below the pump energy within a picosecond, we did non-degenerate measurements on TaAs with a 1.55-eV pump and a 1.10-eV probe, and again with a 2.36-eV pump and a 1.55-eV probe. The measurement did not resolve τ_A, but τ_B remained the same as in the degenerate experiments, as shown in Fig. 4(a). This independence of probe wavelength would seem very implausible if the carriers still resided largely at the pump energy, as in Fig. 4(b); in that case, their strong filling of phase space would cause a probe at the pump energy to measure starkly different dynamics than one at lower energy. On the other hand, after electrons have scattered to lower energy [Fig. 4(c)], the degenerate and non-degenerate probes would yield similar results. Lu *et al.*[34] obtained a similar result, with a similar interpretation, in Cd_3As_2 as they lowered the probe energy closer to the Fermi surface.

As these carriers scatter to lower energy, many end up in the Dirac or Weyl cones—as, indeed, they are known to do within a picosecond in $ZrTe_5$[44] and $SrMnBi_2$.[45] They subsequently persist at low energies for a few picoseconds, giving rise to the signal $\Delta r(t)$ on the timescale of τ_B. Their persistence is not obvious *a priori*, but we support it by measuring the complex phase of our signal, $\Delta r(t)$. We express the result in terms of the change in the complex index of refraction, $\Delta n(t)$, where $n = n_r + in_i$. To understand $\Delta n(t)$, recall that the measured reflectance depends on the refractive index evaluated at the probe's frequency; n_i represents absorption, and n_r, refraction. When photoexcitation changes the absorption at *any* frequency, there is a resulting change in Δn_r at the probe frequency due to the Kramers-Kronig relations between n_r and n_i.[53]

The results for TaAs appear in Fig. 4(d), and a similar result for ZrSiS appears in the supplementary material, Sec. S1 and Figs. S1 and S2. The key observation is that from 0.25 ps to 3.6 ps Δn_r is positive, while Δn_i is negative. These signs are the signature of phase-space filling (PSF)—the occupation of states by photoexcited electrons and holes—at energies below the probe energy.[53] PSF reduces the optical absorption at the corresponding energy; since the carriers have a broad thermal distribution, PSF extends even to the probe energy [Fig. 1(c)], causing the observed $\Delta n_i < 0$. The corresponding Kramers-Kronig change to n_r is positive. It is noteworthy that a negative Δn_i and a positive Δn_r were also observed in Cd_3As_2 on a similar time-scale.[33]

After a few picoseconds, the phase of $\Delta n(t)$ changes. At all later times, $\Delta n_i > 0$ and $\Delta n_r < 0$. These signs are characteristics of the other two primary mechanisms by which photoexcitation changes the optical absorption, namely, Drude absorption and band-gap renormalization (BGR);[53] our experiment does not distinguish the two mechanisms. In Drude absorption, the photoexcited electrons and holes increase the free-carrier density, and the optical conductivity, at low energies. In BGR, heating of the lattice reduces the energy-gap between valence and conduction bands. (In Dirac and Weyl materials, though the linearly dispersing bands lack a gap, BGR may influence the gap between the higher-energy, massive bands.) The slowest component of our signal lasts for hundreds of picoseconds, suggesting that it arises from lattice heating and BGR. Moreover, in ZrSiS we were able to measure the decay rate and diffusion coefficient of this signal (see supplementary material Sec. S2 and Fig. S3), which are consistent with thermal transport.

IV. DISCUSSION

We now relate the observed ultrafast response to the low-energy electronic structure of Dirac and Weyl semimetals, particularly to the low density of states near E_F and the linear dispersion. During the few-picosecond τ_B response, photoexcited electrons and holes are recombining. The low density of states slows the recombination considerably by restricting the phase-space for scattering between electron and hole states. In metals, by contrast, recombination is a purely intraband process and proceeds at the much faster rate of electron-electron scattering,[54,55] roughly equivalent to our sub-picosecond τ_A; recombination may be followed by a few-picosecond phase of electronic cooling. The similarity of metals' ultrafast response to those of Dirac and Weyl semimetals thus belies its very different physical origin. Metals, moreover, lack the strong nonlinearities seen in Dirac and Weyl semimetals,[26] limiting their optoelectronic uses.

Though photocarriers in our Dirac and Weyl materials last much longer than in metals, they last a much shorter

time than in some other semimetals. In bismuth—a semimetal with a momentum-space gap—recombination requires the assistance of a high-momentum phonon, and accordingly lasts for 12 to 26 ps.[38] WTe_2, a type-II Weyl semimetal, is similar: in samples with a momentum gap at E_F, $\Delta R(t)$ decays in two parts, with $\tau_B = 5$ to 15 ps.[56,57] In contrast, the linear, Dirac-like dispersion in our materials speeds recombination because it enables low-momentum transitions between electron and hole states. The linear dispersion also ensures that Auger processes (both interband and intraband) automatically satisfy both energy and momentum conservation, provided they occur along a straight line in momentum-space. Similar considerations make Auger recombination very efficient in graphene.[58]

A third key characteristic of Dirac and Weyl semimetals, their lack of an energy gap at the node, is less apparent in the ultrafast response. Opening a gap can shorten the electronic lifetime by increasing the density of states for electron-phonon scattering,[59] but can also lengthen the lifetime by reducing the phase-space available to Auger recombination, as seen in bilayer graphene.[60] Moreover, a nonzero E_F would have much the same effect on the ultrafast response as would a gap: It would slow Auger recombination by restricting its phase-space.

Though we have focused on our materials' similar ultrafast responses, their decay rates do differ by factors of 2 to 3. A number of material-dependent effects can influence these decay rates, including screening by bound electrons,[55] the phonon band-structure,[46] and the size of the Fermi surface. The latter affects screening of electron-electron interactions, the phase-space available to Auger processes, and plasmon emission.

As new Dirac and Weyl semimetals are discovered, whether in the same material families as our samples or in new ones, they will all share the linear dispersion and low density of states near E_F that dictate the ultrafast properties of our samples. Thus, we can anticipate a rapid, two-part ultrafast response, similar to the one that makes the four materials we have studied promising for optoelectronic applications such as terahertz detectors or saturable absorbers. This ultrafast response could be especially useful if combined with the materials' demonstrated large, anisotropic optical nonlinearity,[26] or with any of the materials' remarkable predicted optical properties.[18–22]

SUPPLEMENTARY MATERIAL

See supplementary material for discussion of the signal's complex phase; discussion of the signal at long times; examples of fits of the data to functional forms other than Eq. (1); and additional data taken in a magnetic field.

ACKNOWLEDGMENTS

Work in Santa Clara and Okinawa was supported by the National Science Foundation DMR-1508278 and by the Geoff and Josie Fox Scholarship. Work in Beijing was supported by the National Basic Research Program of China 973 Program (Grant No. 2015CB921303), the National Key Research Program of China (Grant No. 2016YFA0300604), and the Strategic Priority Research Program (B) of Chinese Academy of Sciences (Grant No. XDB07020100). Work in New Orleans was supported by the U.S. Department of Energy under EPSCoR Grant No. DESC0012432 with additional support from the Louisiana Board of Regents. Work in Germany was supported by the Max Plank Institute (MPI) for Microstructure Physics in Halle, the MPI for Solid State Research in Stuttgart, and the Alexander von Humboldt Foundation.

[1]A. A. Burkov, M. D. Hook, and L. Balents, Phys. Rev. B **84**, 235126 (2011).
[2]S. M. Young, S. Zaheer, J. C. Y. Teo, C. L. Kane, E. J. Mele, and A. M. Rappe, Phys. Rev. Lett. **108**, 140405 (2012).
[3]X. Wan, A. M. Turner, A. Vishwanath, and S. Y. Savrasov, Phys. Rev. B **83**, 205101 (2011).
[4]A. A. Burkov and L. Balents, Phys. Rev. Lett. **107**, 127205 (2011).
[5]H. Weng, C. Fang, Z. Fang, B. A. Bernevig, and X. Dai, Phys. Rev. X **5**, 011029 (2015).
[6]S.-M. Huang, S.-Y. Xu, I. Belopolski, C.-C. Lee, G. Chang, B. Wang, N. Alidoust, G. Bian, M. Neupane, C. Zhang, S. Jia, A. Bansil, H. Lin, and M. Z. Hasan, Nat. Commun. **6**, 7373 (2015).
[7]S.-Y. Xu, I. Belopolski, N. Alidoust, M. Neupane, G. Bian, C. Zhang, R. Sankar, G. Chang, Z. Yuan, C.-C. Lee *et al.*, Science **349**, 613 (2015).
[8]B. Q. Lv, H. M. Weng, B. B. Fu, X. P. Wang, H. Miao, J. Ma, P. Richard, X. C. Huang, L. X. Zhao, G. F. Chen *et al.*, Phys. Rev. X **5**, 031013 (2015).
[9]L. X. Yang, Z. K. Liu, Y. Sun, H. Peng, H. F. Yang, T. Zhang, B. Zhou, Y. Zhang, Y. F. Guo, M. Rahn, D. Prabhakaran, Z. Hussain, S.-K. Mo, C. Felser, B. Yan, and Y. L. Chen, Nat. Phys. **11**, 728 (2015).
[10]T. Liang, Q. Gibson, M. N. Ali, M. Liu, R. J. Cava, and N. P. Ong, Nat. Mater. **14**, 280 (2015).
[11]M. N. Ali, J. Xiong, S. Flynn, J. Tao, Q. D. Gibson, L. M. Schoop, T. Liang, N. Haldolaarachchige, M. Hirschberger, N. P. Ong, and R. J. Cava, Nature **514**, 205 (2014).
[12]X. Huang, L. Zhao, Y. Long, P. Wang, D. Chen, Z. Yang, H. Liang, M. Xue, H. Weng, Z. Fang, X. Dai, and G. Chen, Phys. Rev. X **5**, 031023 (2015).
[13]C. Shekhar, A. K. Nayak, Y. Sun, M. Schmidt, I. Nicklas, M. Leermakers, U. Zeitler, Y. Skourski, J. Wosnitza, Z. Liu, Y. Chen, W. Schnelle, H. Borrmann, Y. Grin, C. Felser, and B. Yan, Nat. Phys. **11**, 645 (2015).
[14]M. N. Ali, L. M. Schoop, C. Garg, J. M. Lippmann, E. Lara, B. Lotsch, and S. S. P. Parkin, Sci. Advances **2**, e1601742 (2016).
[15]C. Yesilyurt, S. G. Tan, G. Liang, and M. B. A. Jalil, e-print arXiv:1610.06288.
[16]Y. Sun, Y. Zhang, C. Felser, and B. Yan, Phys. Rev. Lett. **117**, 146403 (2016).
[17]D. E. Kharzeev and H.-U. Yee, Phys. Rev. B **88**, 115119 (2013).
[18]C.-K. Chan, N. H. Lindner, G. Refael, and P. A. Lee, Phys. Rev. B **95**, 041104 (2017).
[19]J. M. Shao and G. W. Yang, AIP Adv. **5**, 117213 (2015).
[20]P. E. C. Ashby and J. P. Carbotte, Phys. Rev. B **89**, 245121 (2014).
[21]Y. Baum, E. Berg, S. Parameswaran, and A. Stern, Phys. Rev. X **5**, 041046 (2015).
[22]O. V. Kotov and Y. E. Lozovik, Phys. Rev. B **93**, 235417 (2016).
[23]Q. Wang, C.-Z. Li, S. Ge, J.-G. Li, W. Lu, J. Lai, X. Liu, J. Ma, D.-P. Yu, Z.-M. Liao, and D. Sun, Nano Lett. **17**, 834 (2017).
[24]N. Yavarishad, T. Hosseini, E. Kheirandish, C. P. Weber, and N. Kouklin, Appl. Phys. Express **10**, 052201 (2017).
[25]C. Zhu, F. Wang, Y. Meng, X. Yuan, F. Xiu, H. Luo, Y. Wang, J. Li, X. Lv, L. He, Y. Xu, Y. Shi, R. Zhang, and S. Zhu, Nat. Commun. **8**, 14111 (2017).
[26]L. Wu, S. Patankar, T. Morimoto, N. L. Nair, E. Thewalt, A. Little, J. G. Analytis, J. E. Moore, and J. Orenstein, Nat. Phys. **13**, 350 (2017).
[27]S. Chi, Z. Li, Y. Xie, Y. Zhao, Z. Wang, L. Li, H. Yu, G. Wang, H. Weng, H. Zhang, and J. Wang, e-print arXiv:1705.05086.
[28]C. Triola, A. Pertsova, R. S. Markiewicz, and A. V. Balatsky, Phys. Rev. B **95**, 205410 (2017).
[29]S. Ebihara, K. Fukushima, and T. Oka, Phys. Rev. B **93**, 155017 (2016).
[30]C.-K. Chan, P. A. Lee, K. S. Burch, J. H. Han, and Y. Ran, Phys. Rev. Lett. **116**, 026805 (2016).

[31]A. Narayan, Phys. Rev. B **94**, 041409 (2016).
[32]Z. Yan and Z. Wang, Phys. Rev. Lett. **117**, 087402 (2016).
[33]C. P. Weber, E. Arushanov, B. S. Berggren, T. Hosseini, N. Kouklin, and A. Nateprov, Appl. Phys. Lett. **106**, 231904 (2015).
[34]W. Lu, S. Ge, X. Liu, H. Lu, C. Li, J. Lai, C. Zhao, Z. Liao, S. Jia, and D. Sun, Phys. Rev. B **95**, 024303 (2017).
[35]C. Zhu, X. Yuan, F. Xiu, C. Zhang, Y. Xu, R. Zhang, Y. Shi, and F. Wang, Appl. Phys. Lett. **111**, 091101 (2017).
[36]S. Gilbertson, G. L. Dakovski, T. Durakiewicz, J.-X. Zhu, K. M. Dani, A. D. Mohite, D. Andrew, and G. Rodriguez, J. Phys. Chem. Lett. **3**, 64 (2012).
[37]I. Gierz, J. C. Petersen, M. Mitrano, C. Cacho, I. E. Turcu, E. Springate, A. Stöhr, A. Köhler, U. Starke, and A. Cavalleri, Nat. Mater. **12**, 1119 (2013).
[38]Y. M. Sheu, Y. J. Chien, C. Uher, S. Fahy, and D. A. Reis, Phys. Rev. B **87**, 075429 (2013).
[39]M. Breusing, C. Ropers, and T. Elsaesser, Phys. Rev. Lett. **102**, 086809 (2009).
[40]J. A. Sobota, S. Yang, J. G. Analytis, Y. L. Chen, I. R. Fisher, P. S. Kirchmann, and Z.-X. Shen, Phys. Rev. Lett. **108**, 117403 (2012).
[41]Y. H. Wang, D. Hsieh, E. J. Sie, H. Steinberg, D. R. Gardner, Y. S. Lee, P. Jarillo-Herrero, and N. Gedik, Phys. Rev. Lett. **109**, 127401 (2012).
[42]S. Sim, M. Brahlek, N. Koirala, S. Cha, S. Oh, and H. Choi, Phys. Rev. B **89**, 165137 (2014).
[43]G. Wan, W. Yao, K. Zhang, C. Bao, C. Zhang, H. Zhang, Y. Wu, and S. Zhou, e-print arXiv:1710.00350.
[44]G. Manzoni, A. Sterzi, A. Crepaldi, M. Diego, F. Cilento, M. Zacchigna, P. Bugnon, H. Berger, A. Magrez, M. Grioni, and F. Parmigiani, Phys. Rev. Lett. **115**, 207402 (2015).
[45]Y. Ishida, H. Masuda, H. Sakai, S. Ishiwata, and S. Shin, Phys. Rev. B **93**, 100302(R) (2016).
[46]R. Lundgren and G. A. Fiete, Phys. Rev. B **92**, 125139 (2015).
[47]K. Bhargavi and S. Kubakaddi, Phys. Status Solidi RRL **10**, 248–252 (2016).
[48]L. M. Schoop, M. N. Ali, C. Straßer, T. Andreas, V. Andrei, D. Marchenko, V. Duppel, S. S. Parkin, B. V. Lotsch, and C. R. Ast, Nat. Commun. **7**, 11696 (2016).
[49]J. Y. Liu, J. Hu, Q. Zhang, D. Graf, H. B. Cao, S. M. A. Radmanesh, D. J. Adams, Y. L. Zhu, G. F. Cheng, X. Liu, W. A. Phelan, J. Wei, M. Jaime, F. Balakirev, D. A. Tennant, J. F. DiTusa, I. Chiorescu, L. Spinu, and Z. Q. Mao, Nat. Mater. **16**, 905 (2017).
[50]N. Gedik and J. Orenstein, Opt. Lett. **29**, 2109 (2004).
[51]J. Buckeridge, D. Jevdokimovs, C. R. A. Catlow, and A. A. Sokol, Phys. Rev. B **93**, 125205 (2016).
[52]C. Zhang, Z. Yuan, S. Xu, L. Z. B. Tong, M. Z. Hasan, J. Wang, C. Zhang, and S. Jia, e-print arXiv:1502.00251v1.
[53]D. C. Hutchings, M. Sheik-Bahae, D. J. Hagan, and E. W. Van Stryland, Opt. Quantum Electron. **24**, 1 (1992).
[54]J. Hohlfeld, S.-S. Wellershoff, J. Güdde, U. Conrad, V. Jähnke, and E. Matthias, Chem. Phys. **251**, 237 (2000).
[55]N. Del Fatti, C. Voisin, M. Achermann, S. Tzortzakis, D. Christofilos, and F. Vallée, Phys. Rev. B **61**, 16956 (2000).
[56]Y. M. Dai, J. Bowlan, H. Li, H. Miao, S. F. Wu, W. D. Kong, Y. G. Shi, S. A. Trugman, J.-X. Zhu, H. Ding, A. J. Taylor, D. A. Yarotski, and R. P. Prasankumar, Phys. Rev. B **92**, 161104(R) (2015).
[57]B. He, C. Zhang, W. Zhu, Y. Li, S. Liu, X. Zhu, X. Wu, X. Wang, H.-H. Wen, and M. Xiao, Sci. Rep. **6**, 30487 (2016).
[58]T. Winzer, A. Knorr, and E. Malic, Nano Lett. **10**, 4839 (2010).
[59]P. Narang, L. Zhao, S. Claybrook, and R. Sundararaman, Adv. Opt. Mater. **5**, 1600914 (2017).
[60]I. Gierz, M. Mitrano, J. C. Petersen, C. Cacho, I. C. E. Turcu, E. Springate, A. Söthr, A. Köhler, U. Starke, and A. Cavalleri, J. Phys.: Condens. Matter **27**, 164204 (2015).